Fast Algorithm for Determining Eye-Diagram Characteristics of Lossy Transmission Lines

Jeng-Hau Lin, Wei-Da Guo, Guang-Hwa Shiue, Chien-Min Lin, Tian-Wei Huang, and Ruey-Beei Wu

Department of Electrical Engineering and Graduate Institute of Communication Engineering,
National Taiwan University, Taipei, Taiwan, 10617, R.O.C.
Tel: +886-2-23635251 x 340 Fax: +886-2-23638247 E-mail: rbwu@ew.ee.ntu.edu.tw

*Backend Technology Development Division, Taiwan Semiconductor Manufacturing Co., Ltd.

Abstract

A novel algorithm for fast and accurately determining the height and width of eye diagrams at the receiving ends of transmission lines is proposed. While the two parameters concerned in the conductive and dielectric losses in response to the impulse stimulus are derived, the transfer function associated with the propagation coefficient to represent the signaling mechanism on the eye diagram can be developed. A systematic flow is implemented to acquire the predictable eye diagrams in a good agreement with the analysis results by the time-domain circuit simulator for varying designed geometries.

1. Introduction

The eye diagram at the receiving ends of transmission lines is the performance metric of signal integrity analyses for the high-speed interconnection. Design specifications are defined in an eye mask for the timing and voltage margins at the testing points on the channel to gauge the signaling tolerance in the time-domain simulation. Three analysis schemes, the full-wave simulation, macro-model, and signal processing, are usually used to generate the eye diagram in response to the input signal pattern of a pseudo-random bit sequence (PRBS) [1]. Although the shortest length of PRBS is with 127 bits, it is still time-consuming for the full-wave simulation. The procedure to construct a macro-model is also less comprehensible with the physical mechanism of lossy lines. In this paper, the relationship of mechanism between the lossy line and impulse response is thereof exploited.

When transforming the transfer function of frequency-dependant transmission lines to the time domain, two key characteristics of conductive and dielectric losses controlling the respondent behavior of impulse stimuli are investigated. By the convolution of PRBS patterns with various combinations of two designed parameters, the eye diagrams of different transmission-lines are acquired to measure the eye-opening signal integrity in a systematic flow.

2. Analysis Method

A. Transfer Function

For a microstrip structure as depicted in Fig. 1(a), its transmission-line model is known as a series of cells and each of them has the four equivalent elements as shown in Fig. 1(b). The characteristic resistance (R) and conductance (G) vary with the frequency (ω) are respectively given by

$$R = R_s\sqrt{j\omega} \quad \text{and} \quad G = G_d \cdot \omega, \tag{1}$$

where $R_s = \sqrt{\mu_0}/(W\sqrt{\sigma})$ and $G_d = C\cdot\tan\delta$. Considering the length of 'len' for a transmission-line with the propagation coefficient (γ), its transfer function in a match case is given by

$$\mathrm{H}(\omega) \equiv \mathrm{e}^{-\sqrt{(R+j\omega L)(G+j\omega C)}\cdot \mathrm{len}} = \mathrm{e}^{-\gamma\cdot\mathrm{len}}. \tag{2}$$

It is noted that the propagation coefficient can be approximated by [2]

$$\gamma = \sqrt{(R+j\omega L)(G+j\omega C)} \approx j\omega\sqrt{LC} + \frac{R}{2}\sqrt{\frac{C}{L}} + \frac{G}{2}\sqrt{\frac{L}{C}} \tag{3}$$

and thus the transfer function is divided into three parts related to the time delay, conductive loss, and

dielectric loss as read by

$$H(\omega) = \exp(-j\omega\sqrt{LC}\cdot len)\cdot\exp(-0.5R_s\sqrt{j\omega}\cdot\sqrt{C/L}\cdot len)\cdot\exp(-0.5G_d\omega\cdot\sqrt{L/C}\cdot len) \quad (4)$$

B. Impulse Response

Applying the Fourier transform on the three parts of (4) separately can obtain three time-domain impulse responses to be combined by the convolution as given by

$$\mathrm{h}(t) = [\delta(t-t_0)] * [\frac{A}{\sqrt{t^3}\cdot e^{\frac{A^2}{t}}}\cdot \mathrm{u}(t)] * [\frac{2\cdot c}{\pi\cdot(c^2+t^2)}\mathrm{u}(t)], \quad (5)$$

where

$$t_0 = \sqrt{LC}\cdot \mathrm{len}, \qquad A = \frac{R_s}{4}\sqrt{\frac{C}{\pi\cdot L}}\cdot \mathrm{len}, \qquad \text{and} \qquad c = \frac{G_d}{2}\sqrt{\frac{L}{C}}\cdot \mathrm{len}. \quad (6)$$

As noted in (5), the first part becomes a delta function with the time delay (t_0), the transformation of the second part in (4) is referred to [3], and the third part in (4) is transformed through the complex integral.

C. A_n-c_n Diagram

As recalled in (6), the unit of parameter 'A' is the square root of second and the unit of parameter 'c' is the second. To be for the dimensionless convenience, they can be normalized to the pulse width or unit interval (UI) of input stimuli as read, respectively, by

$$A_n = \frac{A}{\sqrt{\mathrm{UI}}} \qquad \text{and} \qquad c_n = \frac{c}{\mathrm{UI}}. \quad (7)$$

Varying the A_n-c_n parameters indicates the changes of physical structures of transmission-lines with the different conductive and dielectric losses in response to the input signal patterns. While fed in the PRBS stimuli, the impulse response of lossy lines through the signaling convolution demonstrates the eye-diagram realization in its corresponding signal integrity. The family curves of A_n-c_n diagrams contour the eye-opening heights and widths as shown in Fig. 2. It is noticed that the exemplar plots are with the percentage while it is normalized to the half of applied maximum voltage and UI, respectively, of input signal patterns.

3. Numerical Results

In reference to the flow chart in Fig. 3, the first step is to extract the S_{21} parameters of lossy lines and then characterize their A_n-c_n parameters by regressing the magnitudes in dB as derived from

$$20\cdot\log_{10}(H(\omega)) = -[20\cdot\log_{10}(e)\cdot UI\cdot c_n]\cdot\omega - [40\cdot\log_{10}(e)\cdot\sqrt{\pi}\cdot\sqrt{UI}\cdot A_n]\cdot\sqrt{\omega}. \quad (8)$$

Nine cases of transmission-line structures along with their corresponding A_n-c_n parameters as listed in Table I are analyzed to verify the proposed algorithm.

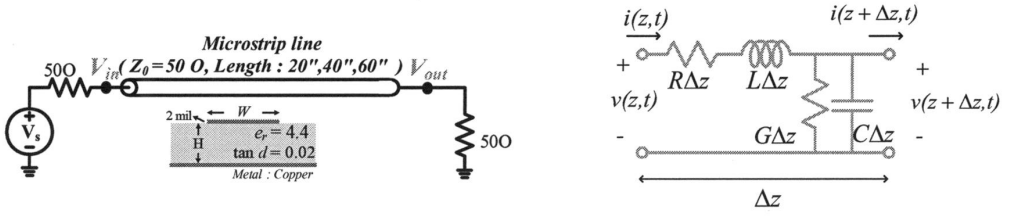
While the input signal of 127-bit PRBS with the rising time of 20ps at 5Gb/s and peak voltage of 0.8V is driven into the lossy line as depicted in Fig. 1(a), the analysis results by the proposed algorithm in comparison with those of HSPICE simulations [4] are demonstrated in Figs. 4, 5 and 6 for Cases 1, 5 and 9, respectively. The quantity data and error percentages of eye-opening heights and widths for nine cases by using HSPICE versus the proposed algorithm are summarized in Table II to be in a good agreement as verified within the deviation of 7.1%.

4. Conclusions

Based on the transfer function of lossy lines, the proposed algorithm achieves in the realization of physical mechanism and the capability of eye-opening prediction rather than applying the time-consuming circuit simulator. Both the impulse response of PRBS patterns and the sensitivity of design structures are characterized in light of A_n-c_n family curves. Further to the demonstrated flow chart, this fast and accurate algorithm can be used to the signal integrity analysis for inter-symbol interference, jitter, and noise margins of high-speed interconnect designs.

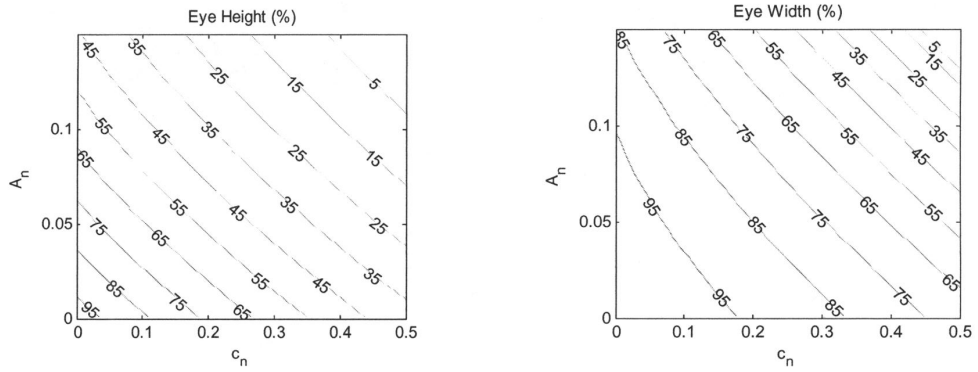
References

[1] K.-C. Zeng, C.-H. Yang, D.-T. Wei, and T. R. N. Rao, "Pseudorandom bit generators in stream-cipher cryptograph," *IEEE Computer*, vol. 24, pp. 8-17, Feb. 1991.
[2] N. N. Rao, *Elements of Engineering Electromagnetics*, 6th ed., Chap. 7 and 12, Englewood Cliffs, New Jersey: Prentice-Hall, 1977.
[3] R. E. Matick, *Transmission Lines for Digital and Communication Networks: An Introduction to Transmission Lines, High-Frequency and High-Speed Pulse Characteristics and Applications*, pp. 122-127 and pp. 195-204, New York: McGraw-Hill, 1969.
[4] HSPICE, Synopsys, Inc. (www.synopsys.com).



(a) Schematic structure. (b) Equivalent transmission-line model.

Fig. 1. Microstrip configuration.



(a) Eye-opening height contour plot. (b) Eye-opening width contour plot.

Fig. 2. Family curves of A_n-c_n diagrams.

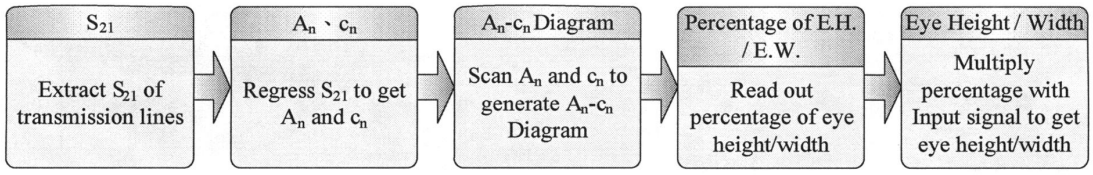
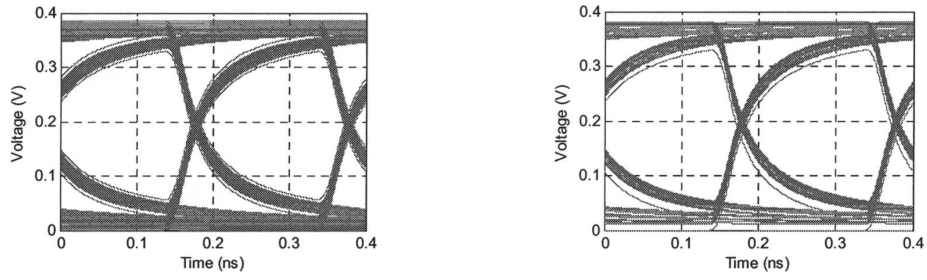
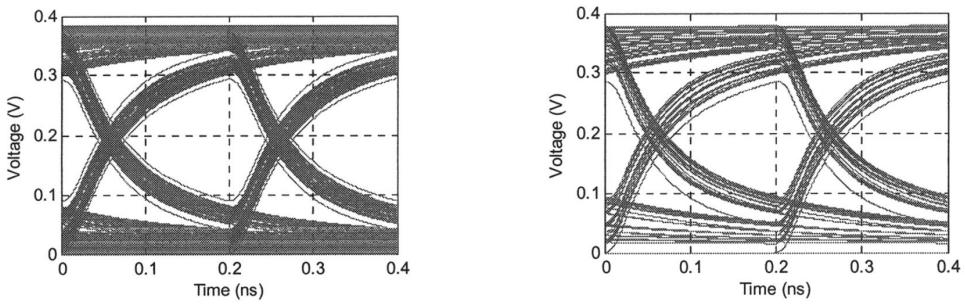


Fig. 3. Flow chart of the proposed algorithm.



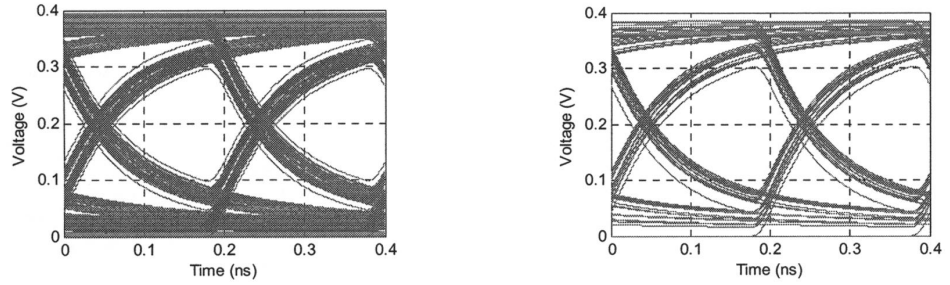
(a) Simulation by the proposed algorithm. (b) Simulation by HSPICE.

Fig. 4. Eye-diagram validation of Case 1 in Table II.



(a) Simulation by the proposed algorithm. (b) Simulation by HSPICE.

Fig. 5. Eye-diagram validation of Case 5 in Table II.



(a) Simulation by the proposed algorithm. (b) Simulation by HSPICE.

Fig. 6. Eye-diagram validation of Case 9 in Table II.

Table I. Dimension settings and A_n-c_n parameters of microstrip lines in Fig. 1.

Case #	len (inch)	Height (H)	Width (W)	A_n	c_n
1	20	5 mil	8.17 mil	0.040	0.110
2		10 mil	17.5 mil	0.023	0.112
3		40 mil	76.8 mil	0.005	0.115
4	40	5 mil	8.17 mil	0.081	0.219
5		10 mil	17.5 mil	0.047	0.224
6		40 mil	76.8 mil	0.010	0.230
7	60	5 mil	8.17 mil	0.121	0.329
8		10 mil	17.5 mil	0.070	0.337
9		40 mil	76.8 mil	0.015	0.344

Table II. Eye-diagram analysis by HSPICE's simulation versus the proposed algorithm's result.

Case		Microstrip in Fig. 1		Eye-Opening Height			Eye-Opening Width		
#	len	Height	Width	HSPICE's	Algorithm's	Error	HSPICE's	Algorithm's	Error
1	20"	5 mil	8.17 mil	278.30 mV	272.64 mV	-2.0%	188 ps	188 ps	0%
2		10 mil	17.5 mil	299.54 mV	299.14 mV	-0.1%	192 ps	192 ps	0%
3		40 mil	76.8 mil	332.47 mV	329.60 mV	-0.9%	197 ps	195 ps	-1.0%
4	40"	5 mil	8.17 mil	143.20 mV	148.34 mV	3.6%	146 ps	149 ps	2.1%
5		10 mil	17.5 mil	193.46 mV	201.48 mV	4.1%	166 ps	168 ps	1.2%
6		40 mil	76.8 mil	267.64 mV	266.58 mV	-0.4%	185 ps	182 ps	-1.6%
7	60"	5 mil	8.17 mil	38.41 mV	41.14 mV	7.1%	63 ps	67 ps	6.3%
8		10 mil	17.5 mil	103.70 mV	107.50 mV	3.7%	116 ps	120 ps	3.4%
9		40 mil	76.8 mil	219.34 mV	212.29 mV	-3.2%	169 ps	165 ps	-2.4%